

# NUMERICAL ANALYSIS OF $SO(10)$ MODELS WITH FLAVOUR SYMMETRIES



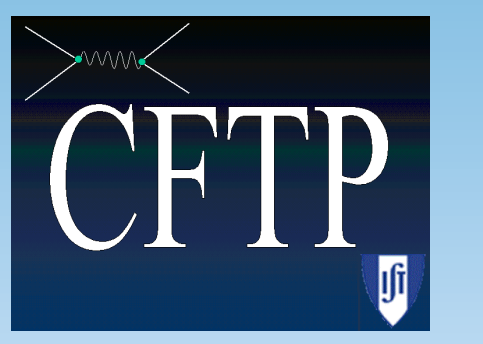
D. Jurčiukonis<sup>(1)</sup>, P. M. Ferreira<sup>(2)</sup>, W. Grimus<sup>(3)</sup>, L. Lavoura<sup>(4)</sup>

<sup>(1)</sup> Vilnius University, Institute of Theoretical Physics and Astronomy, Lithuania

<sup>(2)</sup> ISEL—Instituto Superior de Engenharia de Lisboa, Instituto Politécnico de Lisboa, Portugal

<sup>(3)</sup> University of Vienna, Faculty of Physics, Austria

<sup>(4)</sup> CFTP, Instituto Superior Técnico, Universidade de Lisboa, Portugal



## 1 THE MODEL

$SO(10)$  is a popular gauge group for the construction of Grand Unified Theories (GUTs). The reason is that its 16-plet accommodates at once all the chiral fields of one fermion family. However, inconsistencies in the fit of the experimental masses and mixings of the fermions led to the inclusion of the 120-plet; the resulting theory has been called [1] the “new minimal supersymmetric  $SO(10)$  GUT” (NMSGUT).

However, adding a 120-plet leads to a proliferation of parameters in the Yukawa couplings; one might want to restrict the number of parameters in order to obtain potentially predictive scenarios [2].

The relevant fermion mass matrices are given by

$$M_d = k_d H + \kappa_d G + v_d F, \quad (1a)$$

$$M_u = k_u H + \kappa_u G + v_u F, \quad (1b)$$

$$M_\ell = k_\ell H + \kappa_\ell G - 3v_\ell F, \quad (1c)$$

$$M_D = k_w H + \kappa_D G - 3v_w F, \quad (1d)$$

where  $M_d$ ,  $M_u$ , and  $M_\ell$  are the mass matrices of the down-type quarks, the up-type quarks, and the charged leptons, respectively, while  $M_D$  is the neutrino Dirac mass matrix. The Yukawa-coupling matrices  $H$ ,  $G$ , and  $F$  are associated with the scalar irreps **10**, **120**, and **126**, respectively.

The coefficients  $k_d$ ,  $v_d$ ,  $\kappa_d$ , and  $\kappa_\ell$  are the vacuum expectation values (VEVs) of the Higgs doublet components in the respective  $SO(10)$  scalar irreps which contribute to the Higgs doublet  $H_d$  of the Minimal Supersymmetric Standard Model (MSSM). The remaining coefficients (namely,  $k_u$ ,  $v_u$ ,  $\kappa_u$ , and  $\kappa_D$ ) refer to  $H_u$ . The light-neutrino mass matrix is obtained as

$$M_\nu = M_L - M_D M_R^{-1} M_D^T \quad (2)$$

with  $M_L = w_L F$  and  $M_R = w_R F$ , where  $w_L$  and  $w_R$  are the VEVs of the scalar triplets of the Pati-Salam group  $SU(4)_C \times SU(2)_L \times SU(2)_R$ , which are a part of the scalar 126-plet of  $SO(10)$ .

The “Hermitian mass matrices” are diagonalized as

$$U_d^\dagger (M_d M_d^\dagger) U_d = \text{diag}(m_d^2, m_d^2, m_d^2), \quad (3a)$$

$$U_u^\dagger (M_u M_u^\dagger) U_u = \text{diag}(m_u^2, m_u^2, m_u^2), \quad (3b)$$

$$U_\ell^\dagger (M_\ell M_\ell^\dagger) U_\ell = \text{diag}(m_\ell^2, m_\ell^2, m_\ell^2), \quad (3c)$$

$$U_\nu^\dagger (M_\nu M_\nu^\dagger) U_\nu = \text{diag}(m_1^2, m_2^2, m_3^2), \quad (3d)$$

where the matrices  $U_{d,u,\ell,\nu}$  are unitary and  $|m_3^2 - m_2^2| \gg |m_2^2 - m_1^2| > 0$ . The resulting fermion mixing matrices are

$$V \equiv U_{CKM} = U_d^\dagger U_u, \quad \text{and} \quad U_{PMNS} = U_\ell^\dagger U_\nu. \quad (4)$$

The neutrino mass spectrum is dubbed “normal” if  $m_3^2 > m_2^2$  and “inverted” otherwise.

Three important neutrino mass parameters are

$$m_{\beta\beta} \equiv \left| \sum_{j=1}^3 m_j (U_{PMNS})_{1j} \right|^2, \quad m_{\text{cosmological}} \equiv \sum_{j=1}^3 m_j, \quad (5)$$

$$m_{\text{tritium}} \equiv \left| \sum_{j=1}^3 m_j^2 (U_{PMNS})_{1j} \right|^2.$$

Indeed,  $m_{\beta\beta}$  is potentially measurable in experiments on neutrinoless double-beta decay,  $m_{\text{tritium}}$  may be measured in experiments on the energy end-point of the beta decay of tritium, and  $m_{\text{cosmological}}$  is an important quantity in the calculation of cosmological observables.

Assuming that (a) all three matrices  $H$ ,  $F$ , and  $G$  are nonzero, (b)  $\det F \neq 0$ , and (c) there are no decoupled generations (experimental fact), we have obtained 14 inequivalent cases of Yukawa coupling matrices. 13 cases are generated by  $Z_n$  symmetries (with a suitable  $n$ ), and one case is generated by the  $Z_2 \times Z_2$  symmetry [2].

## 2 NUMERICAL ANALYSIS

The terms  $M_x M_x^\dagger$  (where  $x = d, u, \ell$ ) should fit 13 observables: nine charged-fermion masses and four observables in the CKM matrix. If considered, the term  $M_\nu M_\nu^\dagger$  has to fit 5 additional parameters: three lepton mixing angles, the ratio  $r_{\text{solar}}^2 \equiv (m_2^2 - m_1^2) / (m_3^2 - m_1^2)$ , and the value of  $|m_3^2 - m_2^2|$ . We have used a fixed value  $|m_3^2 - m_2^2| = 2.5 \times 10^{-15} \text{ MeV}^2$ , which allows us to determine the overall scale of  $M_\nu$ , viz.  $|v_d/w_R|$ .

### 2.1 MINIMIZATION FUNCTION

In order to test the viability of each case, and to find adequate numerical values for its parameters, we construct a  $\chi^2$  function

$$\chi^2(x) = \sum_{i=1}^n \left\{ H[f_i(x) - \bar{O}_i] \left( \frac{f_i(x) - \bar{O}_i}{\delta_{\pm} O_i} \right)^2 + H[\bar{O}_i - f_i(x)] \left( \frac{\bar{O}_i - f_i(x)}{\delta_{\pm} O_i} \right)^2 \right\}, \quad (6)$$

where  $n$  is the total number of the observables to be fitted (masses and the mixing parameters). Here  $H$  is the Heaviside step function,  $\bar{O}_i$  is the central value of each observable  $O_i$ ,  $\delta_{\pm} O_i$  are the upper and lower errors of that observable, and  $f_i(x)$ ,  $x = \{x_\alpha\}$ , is the value of the observable in the probed case  $x$ . The data are fitted by minimizing  $\chi^2(x)$  with respect to  $\{x_\alpha\}$ .

The values of the charged-fermion masses, renormalized at  $M_{\text{GUT}} = 2 \times 10^{16} \text{ GeV}$ , are taken from ref. [3]. The used values of the CKM mixing angles [4] are at low-energy scale; we have multiplied the error bars by a factor of three in order to obtain adequately large intervals. The neutrino-mixing observables are given by the  $3\sigma$  intervals from ref. [5].

In order to assess the fit feasibility of each case, we have first attempted to fit only the charged-fermion masses, then the charged-fermion masses together with the parameters of the CKM matrix, and, finally, all that together with the neutrino masses and the PMNS matrix parameters included. The total  $\chi^2$  function is thus the sum of three terms:

$$\chi_{\text{total}}^2 = \chi_{\text{masses}}^2 + \chi_{\text{CKM}}^2 + \chi_{\nu}^2. \quad (7)$$

For the neutrino masses, we have analysed both possibilities of the normal and inverted neutrino mass spectra.

In some cases we could not find a reasonably small value of  $\chi_{\text{masses}}^2$  alone. Further analysis of those cases by considering  $\chi_{\text{CKM}}^2$  and  $\chi_{\nu}^2$  made no sense. Similarly, in some other cases a sufficiently low value of  $\chi_{\text{masses}}^2 + \chi_{\text{CKM}}^2$  could not be achieved, so we did not have to consider  $\chi_{\nu}^2$ . Finally, even if the value of  $\chi_{\text{total}}^2$  could be reasonably low, we still had to check whether the ratio  $|w_R/v_d|$  turned out in the right range. Indeed, since  $v_d$  must be of order of the Fermi scale 100 GeV and  $w_R$  must be of order of the grand-unification scale  $10^{16} \text{ GeV}$ , we must require  $|w_R/v_d|$  to be  $10^{14}$  or even larger.

### 2.2 NUMERICAL METHOD

The minimization of  $\chi^2(x)$  is a difficult task because the various parameters  $x_\alpha$  differ by several orders of magnitude and because of a large number of local minima.

For the numerical minimization of the  $\chi^2$  functions we have employed the Differential Evolution (DE) algorithm. This is a stochastic algorithm that exploits a population of potential solutions in order to effectively probe the parameter space.

The effectiveness of the DE algorithm strongly depends on control parameters. We have performed preliminary tests in order to hand-tune the appropriate ranges for the control parameters in each case. Also, we have adjusted the errors  $\delta_{\pm} O_i$  (within the range of magnitude of the true errors) according to the behaviour of the fits. Repeating the procedure for each case, we have thus been able to test more local minima (defined as the points where the minimization algorithm converges) and to find the minima closer to the global minimum.

All the numerical calculations were implemented by using the programming language Fortran.

### 2.3 NUMERICAL RESULTS

We have found that all the cases, except for the cases A and B, either fail to fit the observables adequately or give a too low value for  $|w_R/v_d|$ . Only the case D<sub>1</sub> is able to fit all the observables, but all those good fits yield  $|w_R/v_d| < 3 \times 10^{13}$ .

We have found that the case B is able to fit perfectly all the observables. This is true irrespective of whether the neutrino mass spectrum is normal or inverted. However, when the neutrino mass spectrum is inverted the value of  $|w_R/v_d|$  is too small.

For a normal neutrino mass spectrum in the case B, on the other hand, there are “fits” (sets of the parameters  $\{x_\alpha\}$ ) in which all the inequalities, connected with the

unification scale, are observed. The value of  $\chi_{\text{total}}^2$  for the best fit is smaller than  $10^{-3}$ , i.e. for all practical purposes it is zero. The neutrino masses for this best fit are following:  $m_1 \approx 6 \times 10^{-3} \text{ eV}$ ,  $m_2 \approx 1 \times 10^{-2} \text{ eV}$ , and  $m_3 \approx 5 \times 10^{-2} \text{ eV}$ . One therefore obtains  $m_{\text{cosmological}} \approx 7 \times 10^{-2} \text{ eV}$ ,  $m_{\text{tritium}} \approx 1 \times 10^{-2} \text{ eV}$ , and  $m_{\beta\beta} \approx 6 \times 10^{-3} \text{ eV}$ .

The case A has much too many degrees of freedom, so it is adequate to try and constrain it somewhat. We follow a proposal of ref. [6], where real Yukawa-coupling matrices (due to an additional  $CP$  symmetry)  $F$ ,  $G$ , and  $H$  are enforced and, moreover,  $w_L = 0$  is assumed, thereby discarding the type-II seesaw mechanism.

We have attempted to fit the case A both to the updated charged-fermion masses of ref. [3] and to the now extant value of  $\sin^2 \theta_{13}$ . We could achieve an excellent fit ( $\chi_{\text{total}}^2 \approx 0.005$ ) when the neutrino mass spectrum is normal and a passable one ( $\chi_{\text{total}}^2 \approx 0.7$ ) when the mass spectrum is inverted. The best fit with the normal hierarchy of the neutrino masses has  $m_{\text{cosmological}} \approx 6 \times 10^{-2} \text{ eV}$ ,  $m_{\text{tritium}} \approx 9 \times 10^{-3} \text{ eV}$ , and  $m_{\beta\beta} \approx 4 \times 10^{-3} \text{ eV}$ . The best fit with the inverted hierarchy of the neutrino mass spectrum has  $m_{\text{cosmological}} \approx 1 \times 10^{-2} \text{ eV}$  and  $m_{\text{tritium}} \approx m_{\beta\beta} \approx 5 \times 10^{-3} \text{ eV}$ .

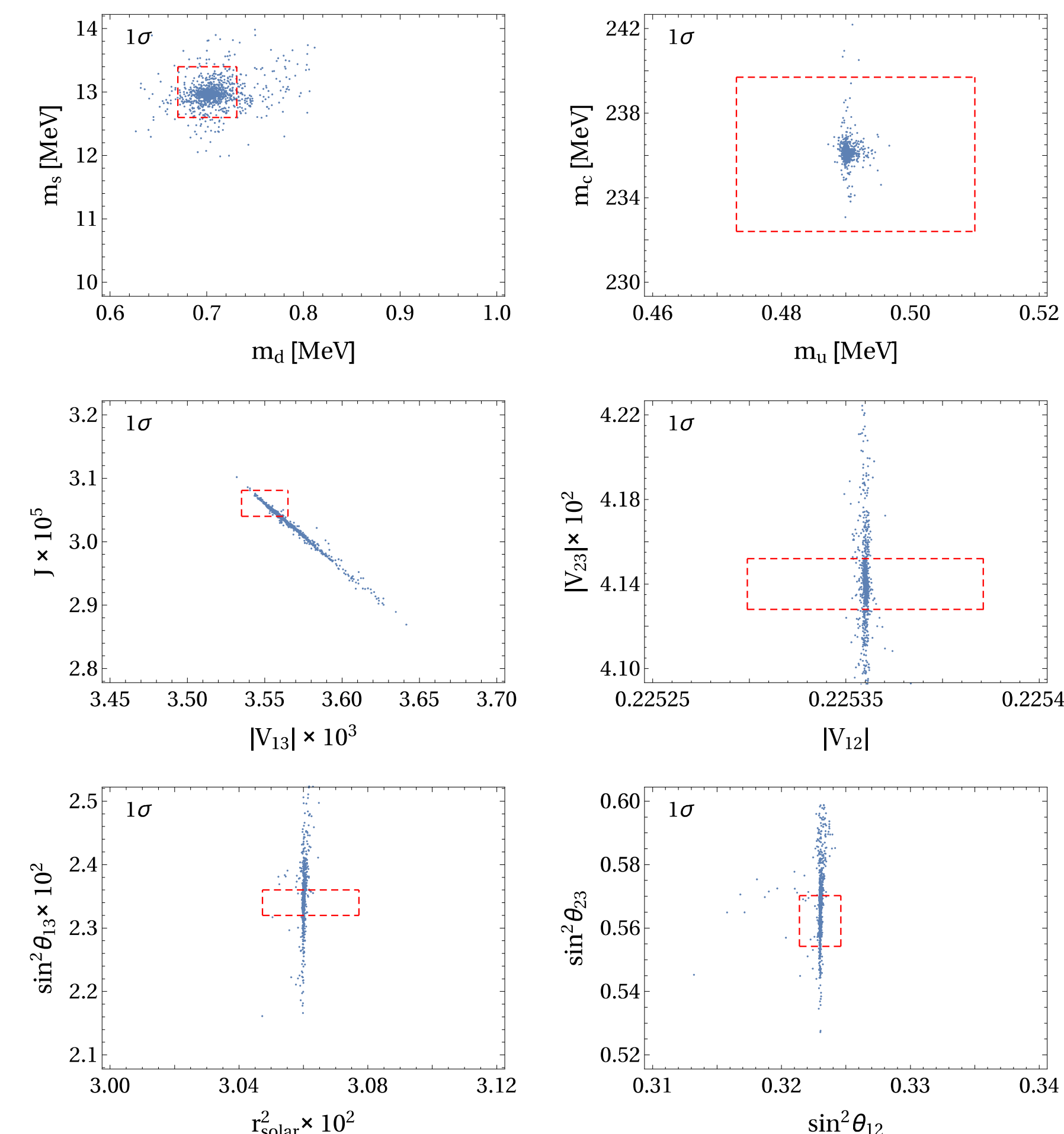


Figure 1: Fits to various observables in the case B with the normal hierarchy of neutrinos. Points in the plots satisfy the  $1\sigma$  experimental boundaries and  $\chi_{\text{total}}^2 \in (3 \times 10^{-4}, 0.99)$  for all fits. The red rectangular denotes the region of  $0.1 \times 1\sigma$  experimental boundaries.

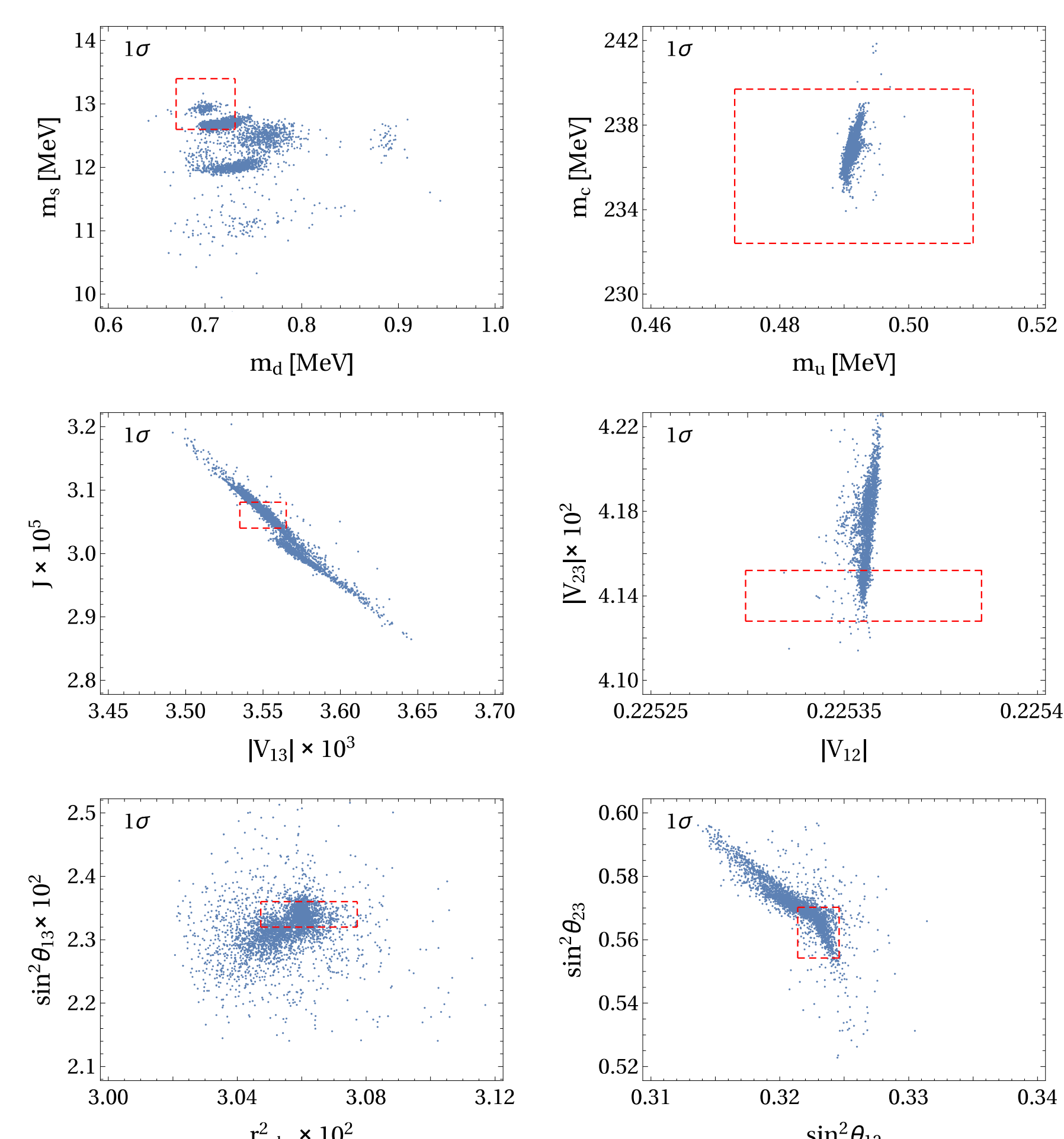


Figure 2: Fits to various observables in the case A with the normal hierarchy of neutrinos. Points in the plots satisfy the  $1\sigma$  experimental boundaries and  $\chi_{\text{total}}^2 \in (0.005, 0.99)$  for all fits. The red rectangular denotes the region of  $0.1 \times 1\sigma$  experimental boundaries.

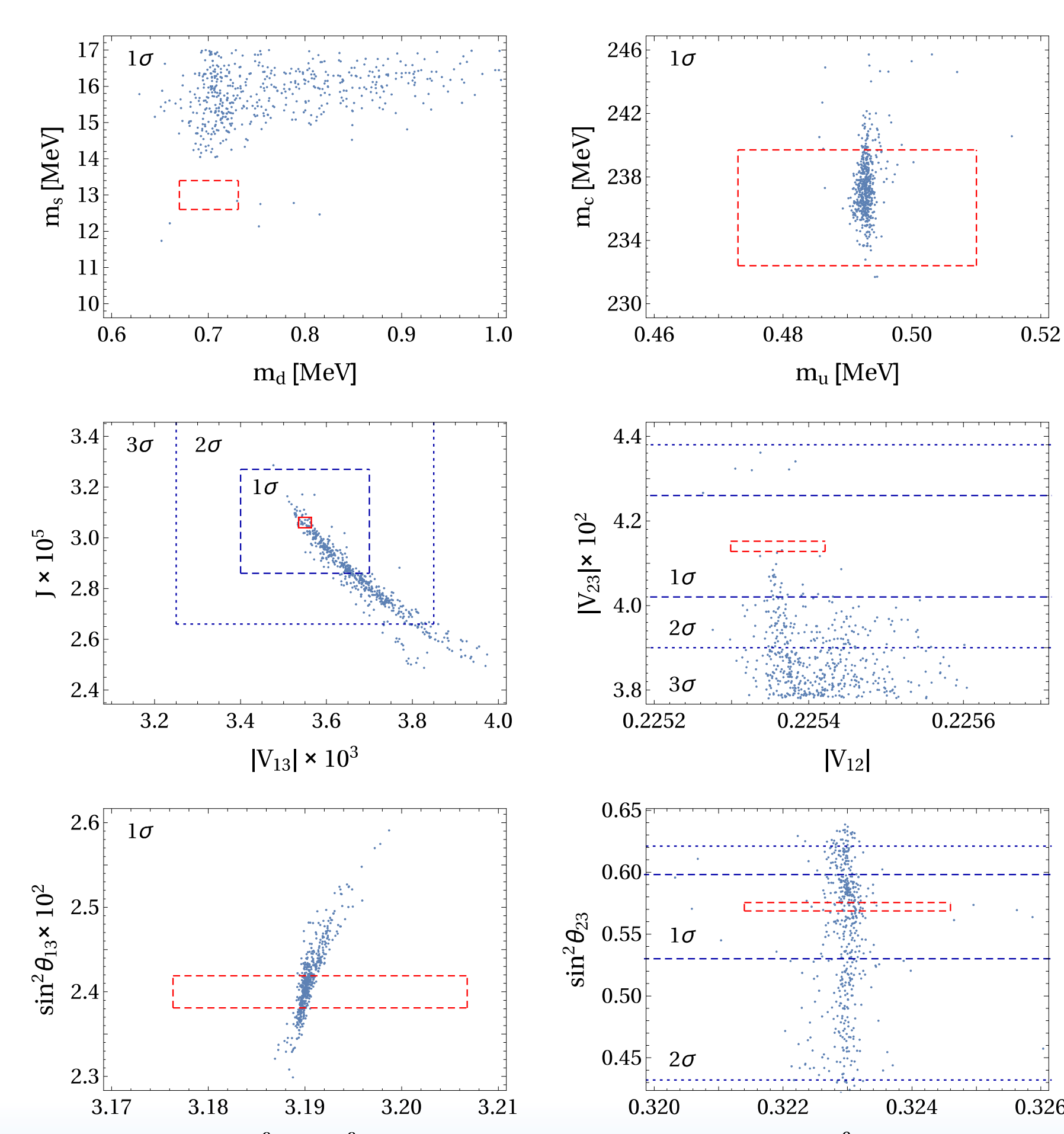


Figure 3: Fits to various observables in the case A with the inverted hierarchy of neutrinos. Points in the plots satisfy the  $3\sigma$  experimental boundaries and  $\chi_{\text{total}}^2 \in (0.7, 4.6)$  for all fits. The red rectangular denotes the region of  $0.1 \times 1\sigma$  experimental boundaries whereas the blue dashed and blue dotted lines denote the  $1\sigma$  and  $2\sigma$  boundaries respectively.

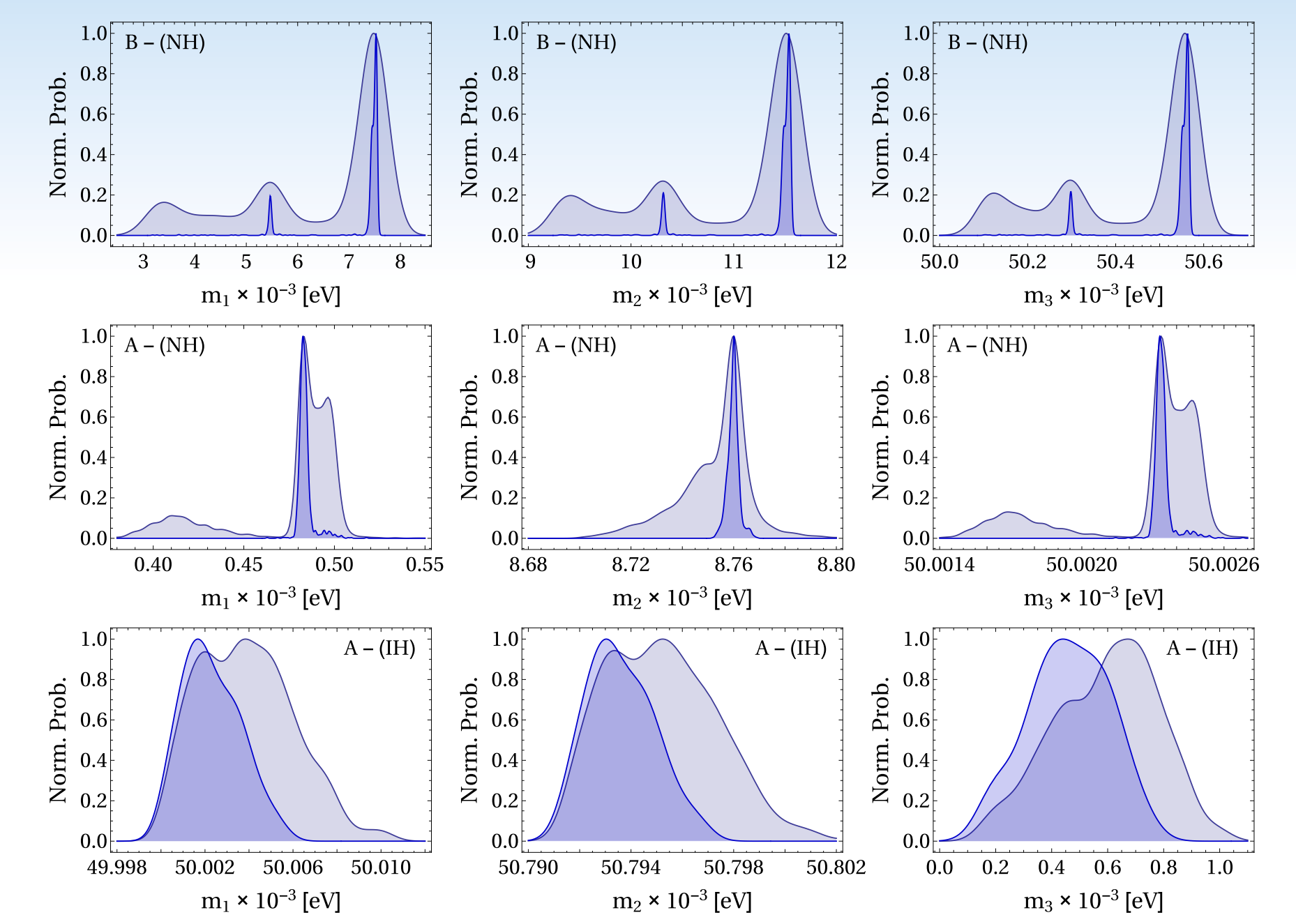


Figure 4: Distributions of the neutrino masses for the cases A and B in the sets of fits presented in Figure 1 – Figure 3. Darker blue areas illustrate distributions of the selected best fits which make 1/4th of the total sets. The  $y$ -axis shows the peak-normalized probability.

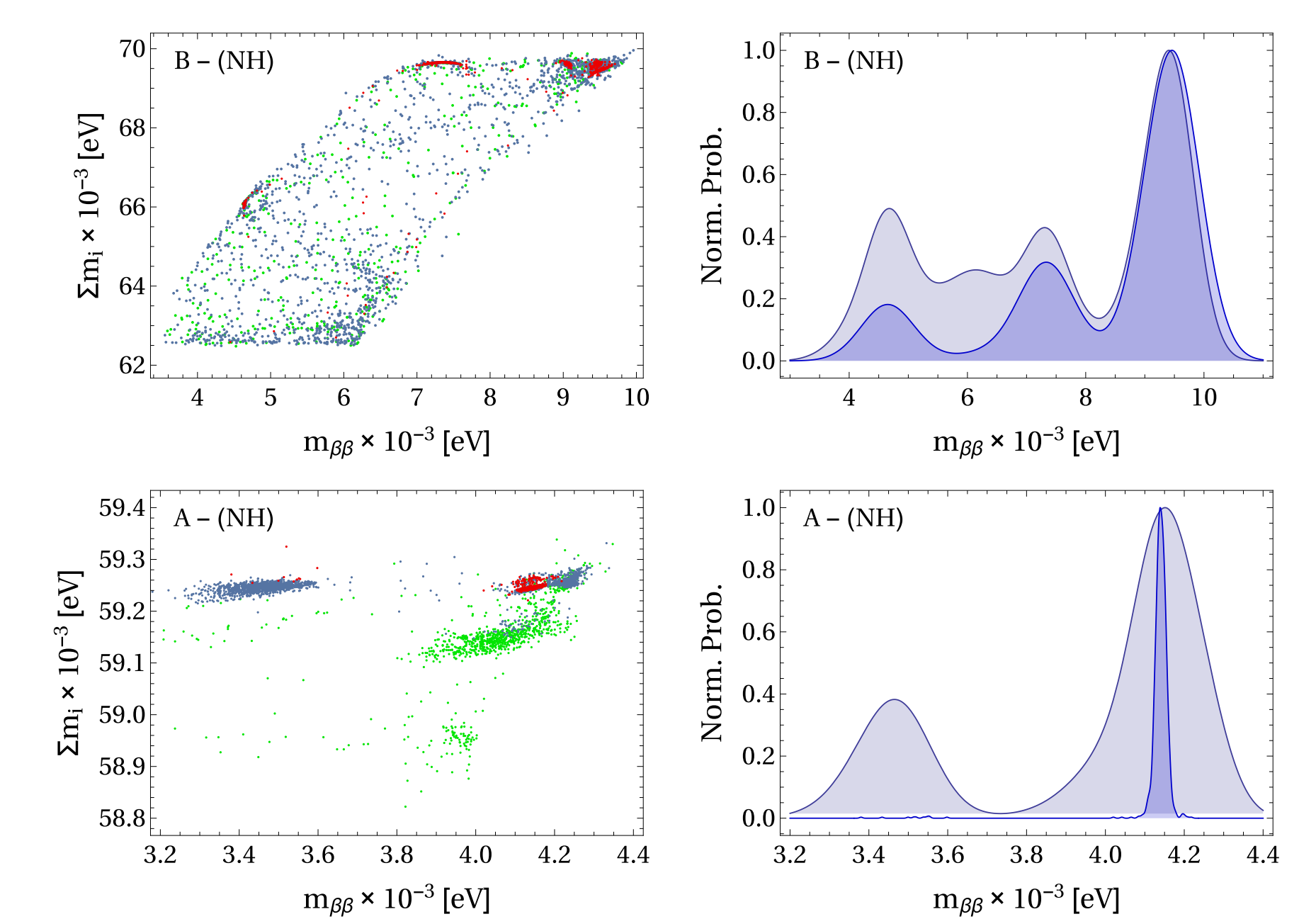


Figure 5: Scatter plots of the  $m_{\beta\beta}$  versus  $m_{\text{cosmological}} = \sum_i m_i$  are shown on the left side, and the corresponding distributions of  $m_{\beta\beta}$  are shown on the right side, for the cases A and B. Red, blue, and green dots show the fits that are selected according to the increasing value of  $\chi_{\text{total}}^2$  and constitute fractions of [1/4, 1/2, and 1/4] of the total set respectively. Darker blue areas illustrate peak-normalized distributions of the best fits which correspond to the red dots in the scatter plots.

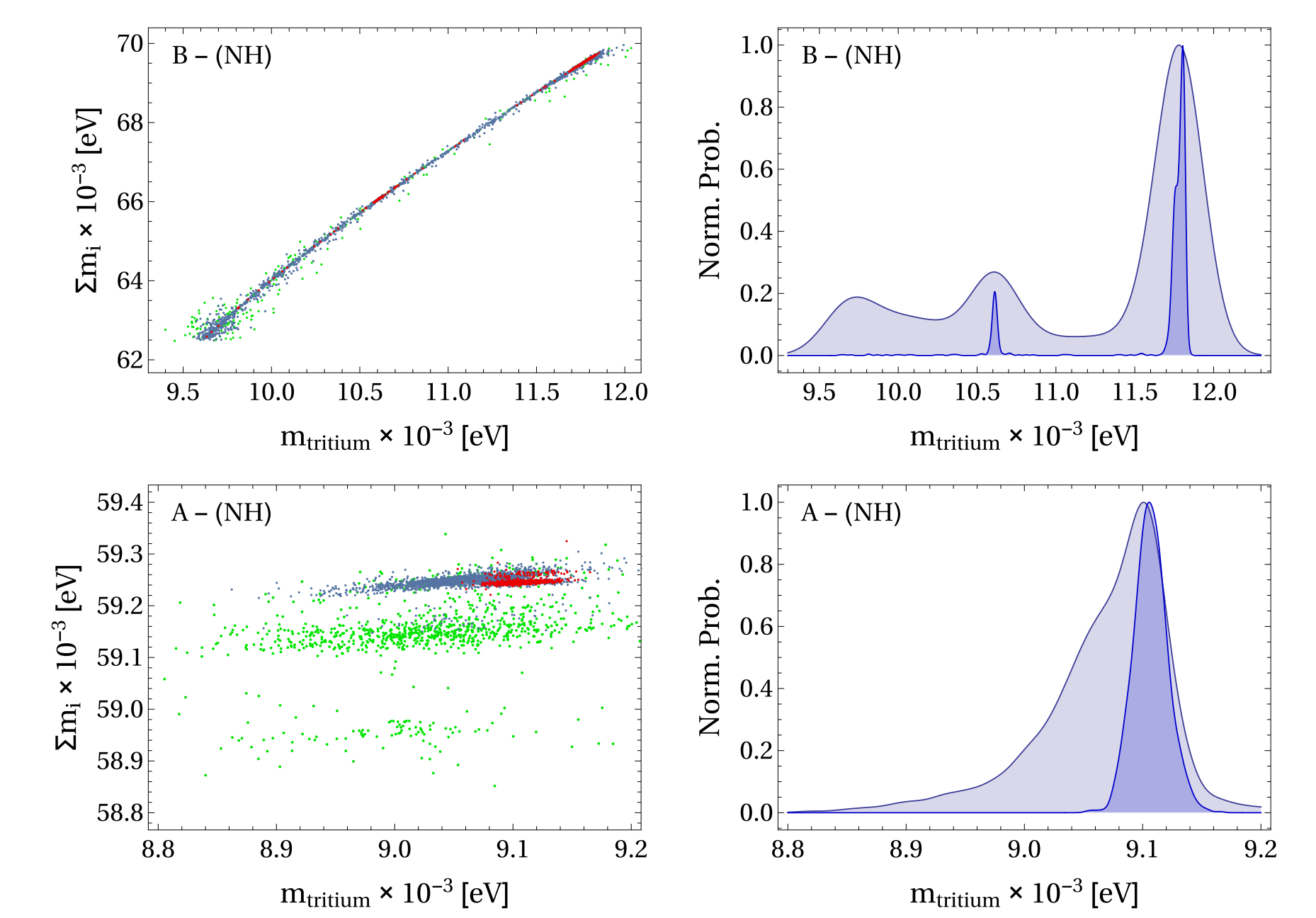


Figure 6: Scatter plots of the  $m_{\text{tritium}}$  versus  $m_{\text{cosmological}} = \sum_i m_i$  are shown on the left side, and the corresponding distributions of  $m_{\text{tritium}}$  are shown on the right side, for the cases A and B. Red, blue, and green dots show the fits that are selected according to the increasing value of  $\chi_{\text{total}}^2$  and constitute fractions of [1/4, 1/2, and 1/4] of the total set respectively. Darker blue areas illustrate peak-normalized distributions of the best fits which correspond to the red dots in the scatter plots.

## 3 CONCLUSIONS

The numerical analysis ruled out all 14 cases except for the case A and the case B. Both cases A and B allow excellent fits to the data when the neutrino mass spectrum is normal: when that spectrum is inverted, the case A can still fit the data but we were unable to find a good fit in the case B. Using parameters of fits we can make predictions for the neutrino sector. Finally, we conclude that within the new minimal supersymmetric  $SO(10)$  GUT (NMSGUT) there are at most two possibilities to reduce the number of Yukawa couplings through flavour symmetries, while remaining in agreement with the data.

## 4 REFERENCES

- [1] C. S. Aulakh and S. K. Garg, Nucl. Phys. B **857** (2012) 101.
- [2] P. Ferreira, W. Grimus, D. Jurčiukonis and L. Lavoura, Nucl. Phys. B **906** (2016) 289.
- [3] Z. Z. Xing, H. Zhang, and S. Zhou, Phys. Rev. D **77** (2008) 113016.
- [4] K. A. Olive *et al.* (Particle Data Group), Chin. Phys. C **38** (2014) 090001.
- [5] D. V. Forero, M. Tórtola, and J. W. F. Valle, Phys. Rev. D **90** (2014) 093006.
- [6] W. Grimus and H. Kühböck, Phys. Lett. B **643** (2006) 182.

